Journal of Neonatal Surgery
ISSN(Online): 2226-0439
Vol. 14, Issue 17s (2025)
https://www.jneonatalsurg.com

OPEN ACCESS

Multi-Task and Multi-Dimensional Deep Learning for Alopecia Areata Detection and Diagnosis

C. Saraswathi[1]

[1]Assistant Professor, Department of Computer Applications, Chikkanna Government Arts College, Tirupur -2. (Deputed from Dept. of Computer & Information Science, Annamalai University)

Email ID: saraswathichinnaiyan@gmail.com

Cite this paper as: C. Saraswathi, (2025) Multi-Task and Multi-Dimensional Deep Learning for Alopecia Areata Detection and Diagnosis. *Journal of Neonatal Surgery*, 14 (17s), 96-107.

ABSTRACT

Unhealthy lifestyles and vitamin deficiencies contribute to various scalp-related issues, such as dermatitis and baldness. Alopecia Areata (AA) is a prevalent form of hair loss, commonly diagnosed using medical image processing-based models. However, these models often struggle with overlapping hairs and are highly sensitive to configuration variables, making them less reliable. To overcome these limitations, deep learning has been increasingly applied in medical image analysis for the detection and diagnosis of AA. While several deep learning models have been developed to recognize different scalp conditions, there remains a need for simultaneous identification of AA and other scalp conditions to improve diagnostic accuracy.This study introduces a Multi-Task Deep (MTDeep) learning system, incorporating the MT Faster Residual Convolutional Neural Network with Long Short-Term Memory (MT-FRCNN-LSTM) model. This approach aims to recognize both AA and various scalp conditions in individuals with different baldness patterns. The primary objective of multi-task learning (MTL) is to improve recognition accuracy through the use of a shared encoder. In this model, scalp and AA images are initially processed through an LSTM encoder and an FRCNN encoder, extracting global and local features at different scales. These extracted features are then fused to generate a comprehensive feature representation. Finally, a fully connected layer, followed by a softmax classifier, is applied to categorize different scalp conditions.

Keywords: *Scalp conditions, Alopecia Areata, Deep learning, FRCNN, LSTM, Multi-task learning*

1. INTRODUCTION

As the Biblical Samson explained to us in Judges 16, hair is a strong physical representation. The hair loss, also known as alopecia represents a loss of influence and domination. A hair loss or scalp hair symptoms are usually the results of a stressful case [1]. Nowadays, many people suffer from scalp hair issues such as dandruff, folliculitis, hair loss and greasy hair due to a variety of factors such as bad daily routines, an unbalanced nutritional intake, excessive stress and poisonous elements in their environments [2]. At least 30% of these issues result in hair loss. Rajput [3] investigated the etiology and clinical manifestations of hair loss caused by air pollution. According to the World Health Organization (WHO), about 70% of individuals have scalp hair issues [4]. Endocrine, genetic, illness, and other internal variables can all contribute to scalp hair issues. Additionally, dandruff, scalp pruritus and related signs occurred in the French people. Many investigations revealed that about 18% of children in the USA and Australia are affected by dandruff. So, both adults and children may have scalp hair issues [5-6]. So, understanding how to successfully avoid scalp hair-related disorders and maintain scalp hair is critical. In recent years, specific treatments, such as scalp hair physiotherapy, have evolved to treat more acute scalp disorders.

Manual inspection is used to assess the state of the patient's scalp hair in the current most popular processing techniques in scalp hair physical treatment [7]. However, such manual diagnostic tests are based on the physiotherapist's competence level, and as a result, they might provide a variety of outcomes and worries about the scalp hair condition and diagnosis. The two major challenges exist associated with hair care services in the recent hairdressing industry are: (i) Due to the regular staffing levels in the hairdressing business, organizations have invested significant time and cost to consistently enhance physiotherapy skillsets; and (ii) Even among professional physiotherapists who have received the same professional training, the interpretation of scalp hair microscope pictures varies. Such discrepancies in diagnostic result interpretation might also be attributed to a lack of expertise.

To combat all these challenges, a deep learning-based intelligent scalp detection and diagnosis model called ScalpEye [8] has been developed to identify and diagnose frequent scalp hair symptoms in scalp healthcare, including dandruff, folliculitis, hair loss and oily hair. This system was comprised of a portable scalp hair imaging microscope, a mobile device app, a cloud-based Artificial Intelligence (AI) training server and a cloud-based administration platform. In this system, the FRCNN with

Inception_ResNet_v2_Atrous model has been chosen as the deep learning training model and employed to identify and diagnose various types of scalp hair symptoms. Among various scalp symptoms, Alopecia Areata (AA) is a common hair loss disorder with a lifetime frequency of around 2% [9] that is distinguished by sudden onset of non-scarring hair loss in generally sharply defined regions [10]. Some people have just a tiny patch of hair loss, whilst others have more widespread or less typically distributed involvement [11]. Many scalp and dermoscopic images have been utilized to recognize and diagnose AA in the past few years. Generally, Tracheoscopies and biopsies are frequently necessary to recognize and diagnose AA as the cause of hair loss [12]. There are many disadvantages to those diagnostic analyses, including the question of how many tests are required for a reliable diagnosis. As a result, there is a lot of space for further research on AA recognition and diagnosis based on the AI models such as machine learning and deep learning approaches [13-15]. Such AI models, including Support Vector Machine (SVM), K-Nearest Neighbor (KNN), decision trees, Artificial Neural Network (ANN), Convolutional Neural Network (CNN), etc., have been applied in a range of healthcare systems for proper diagnostic purposes. In dermatology or trichology, many machine learning and deep learning approaches have been utilized to produce accurate diagnoses and forecasts using healthy and AA hair images [16]. However, it needs simultaneous recognition of AA with the scalp condition to guide proper diagnosis.

Therefore in this paper, an MTDeep learning system is developed based on the MT-FRCNN-LSTM model for identifying AA and scalp conditions together for multiple individuals with the varieties of baldness. This system has the objective of employing an additional shared encoder for increasing the efficiency of identifying AA and scalp conditions. Initially, the scalp and AA hair images are passed to the LSTM encoder and the FRCNN encoder for obtaining the global and local features at different scales. After that, such features are merged to get the final feature vector representation. Further, the fully connected layer followed by the softmax classifier is used to simultaneously recognize the AA and scalp conditions. Thus, this system enhances the accuracy of AA detection and diagnosis effectively.

The remaining sections of this manuscript are prepared as follows: Section II discusses the recent works related to AA/scalp conditions detection and classification. Section III explains the MT-FRCNN-LSTM model and Section IV illustrates its efficiency. Section V concludes the entire study and suggests future enhancement.

2. LITERATURE SURVEY

Nabahhin et al. [17] developed an expert model, which conducts treatment for various probable hair loss disorders of the levels between individuals by asking yes or no questionnaires. First, it may ask the customer to choose the proper answer on all screens. At the end of the dialog session, the treatment and suggestion of the disorder were provided to the customer. On the other hand, more characteristics related to hair loss were needed to improve the diagnosis. Wang et al. [18] applied the deep learning models to hairy scalp images to identify the different scalp conditions. In this model, the ImageNet-VGG-f structure Bag-Of-Words (BOW) was executed with SVM classifier and Histogram-Of-Gradients (HOG) or Pyramid HOG (PHOG) with SVM classifier. But, the number of scalp images for training was inadequate and it needs an ensemble model to increase the detection accuracy.

Lee et al. [19] identified the topographic phenotypes of AA using cluster analysis and designed a grading model to stratify diagnosis. At first, clinical images for patients with AA were collected and reviewed to analyze alopecia using the severity of Alopecia Tool 2. Then, topographic phenotypes of AA were detected by hierarchical clustering with Ward's method. Also, variances in clinical features and diagnosis were compared across the different clusters. But, the statistical efficiency was degraded because of the limited number of patients with severe AA.

Seo & Park [20] presented a scheme to prevent hair loss and diagnose the scalp by capturing Alopecia Feature (AF) depending on the scalp image. Primarily, the scalp images were preprocessed by the image processing to fine-tune the contrast of microscopy input and reduce the light reflection. Then, the AFs like the number of hair, follicles, density, etc., were extracted from the preprocessed images by the gridline selection and eigenvalues to compute the growth level of alopecia. But, it needs a massive quantity of scalp images and designs an AI model to automatically extract several kinds of AFs for increasing efficiency.

Fatima et al. [21] investigated clinical, dermoscopic and histopathological findings in patients of AA. In this investigation, 50 successive patients participating dermatology outpatient department of a tertiary care hospital over 2 years with clinical attributes evocative of AA were chosen. After that, a clinical analysis was conducted by dermoscopy and skin biopsy taken from the margin of an active lesion. Moreover, the data was evaluated by determining the mean and standard variance. However, it needs an automated model to identify and diagnose AA appropriately.

Ibrahim et al. [22] presented an analysis of the pre-trained categorization of scalp conditions with the help of image processing methods. At first, the scalp images were collected and preprocessed. Then, various characteristics like shape, color and texture were obtained from all images to determine the Region-Of-Interest (ROI). The values of the pre-trained features were utilized as a reference during the categorization. The SVM was used to categorize the scalp conditions. But, it needs a deep learning model to increase the feature extraction and classification efficiency.

Zhang et al. [23] developed a rapid and simple technique to identify the level of hair damage based on the lightweight CNN

model called Hair Diagnosis MobileNet (HDM-Net). In this technique, the HDM-Net was utilized to obtain and choose the features. Such features were then fed to the SVM to categorize hair damage images. Though it reduces the number of parameters, its accuracy was not effective.

Shakeel et al. [24] developed a model for the categorization of healthy hairs and AA. First, hair images of healthy and AA conditions were collected and preprocessed for partition. Then, various features such as texture, shape and color were extracted from each segment. Moreover, SVM and KNN classifiers were employed to classify those features into healthy and AA. But, it needs deep learning classifiers to increase the accuracy.

Kim et al. [25] evaluated the efficiency of hair density measurement by employing a deep learning model. First, the hair scalp RGB images were obtained from male alopecia patients. Then, the related annotation data was also acquired that contained the position data of the hair follicles in the image and follicle-sort data based on the number of hairs. Moreover, those images were classified by the EfficientDet, YOLOv4 and DetectoRS to identify the classes of hair follicles. But, the efficiency of all these classifiers for hair follicles of class 3 was poor because the images of class 3 comprise features similar to those in the images of class 1 and class 2. Also, the class imbalance occurred between class 3 and the other classes.

3. III. PROPOSED METHODOLOGY

In this section, the MT-FRCNN-LSTM model is described briefly for identifying and diagnosing AA and scalp conditions in parallel. Figure 1 depicts the schematic representation of this presented MTDeep system. Initially, the hair and scalp images of healthy and AA are acquired from the publicly available databases. Then, those images are applied to train the MT-FRCNN-LSTM model and the trained model is used to categorize the test samples into healthy and different conditions of AA.

3.1 Image Acquisition

In this study, 2 different publicly available databases are gathered and they are:

Figaro1k database: It is an open database comprising 1050 hair images, equally distributed in various classes like straight, wavy and curly [26].

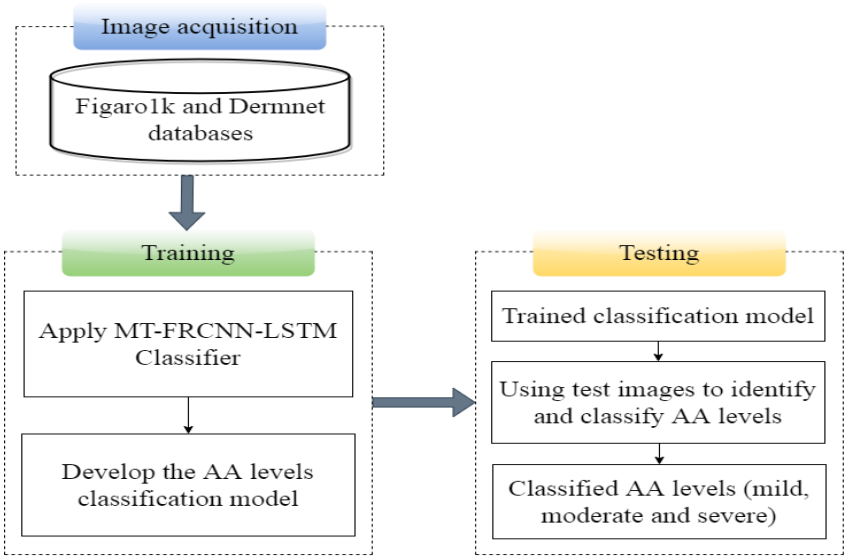

Figure 1. Schematic Representation of Presented MTDeep System for AA and Scalp Symptoms Identification and Diagnosis

Dermnet database: It is an open database accessible on Dermnet, containing 23 classes of dermatological disorders, including AA [27]. A total of 108 images are retrieved for 3 different AA classes: mild, moderate and severe.

The hair and scalp images collected from these databases are given to the MTDeep system for AA conditions identification and diagnosis.

3.2 MTDeep System

The MT-FRCNN-LSTM model is designed to conduct the AA levels identification based on the various scalp conditions. The entire architecture of this model is illustrated in Figure 2.

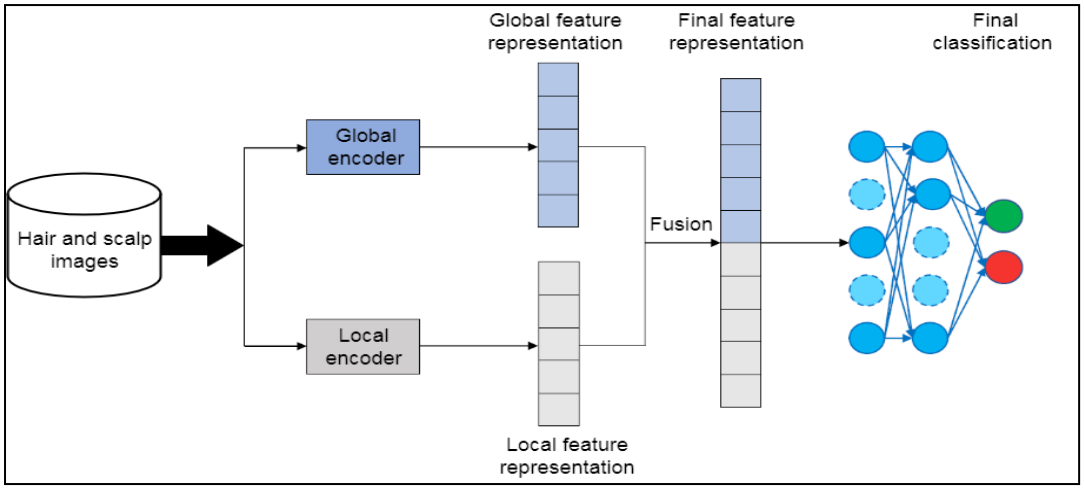

Figure 2. Entire Pipeline of the MT-FRCNN-LSTM Model

This MTDeep system is explained in the following sub-section:

3.2.1 Multi-Task Learning Model

Multi-task learning ensures better efficacy in various image processing and classification processes. Because of the semantic variances among distinct types of scalp conditions, even if the aim is to categorize AA levels, it is suitable for the multi-task learning scheme. This MTDeep system adopts the Adversarial Multi-Task (AMT) learning model and enhances the architecture of its encoder. Adversarial multi-task learning is depending on Global-Local Multi-Task Learning (MTL), as depicted in Figure 3.

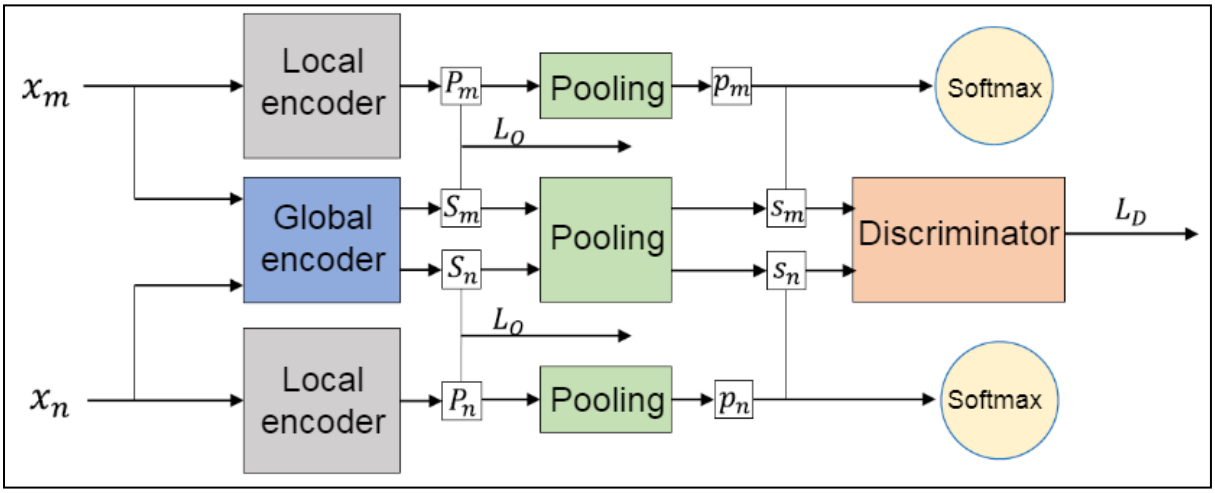

Figure 3. Structure of Adversarial Multi-task Learning Model

For GL-MTL, the hair and scalp images in all databases are allocated to 2 feature spaces to encode: global space and local space. Global encoders are utilized to obtain hair image features that are independent of AA while local encoders are utilized to obtain scalp images that are more relevant to the AA. For an image x_k in every AA class k, the global feature S_k and the local feature P_k of the image are extracted by the 2 encoders. Additionally, the global representation s_k and local representation p_k of the image are acquired after pooling.

Based on the Generative Adversarial Network (GAN), the adversarial MTL attempts to create a global space comprising fewer data than the local space and incorporate a discriminator after the global encoder. It maps the global representation of the image to the probability distribution to estimate which AA class the image comes from, as defined in Eq. (1). During the learning task, the global encoder avoids the discriminator from creating an accurate decision on the AA classification, guaranteeing that the global representation of the image is independent of the classification, whereas the discriminator attempts its best to recognize which AA class the current image feature representation comes from. The discriminator loss l_D is added in the loss function, as defined in Eq. (2).

$$D(s_k, \theta_D) = softmax(b + Us_k) \quad (1)$$

In Eq. (1), $U \in \mathbb{R}^{d \times d}$ denotes the variable that can be learned, $b \in R^d$ denotes the bias and θ_D indicates the variable of the discriminator.

$$l_D = \min_{\theta_S}\left(\lambda \max_{\theta_D}\left(\sum_{k=1}^{K}\sum_{i=1}^{N_k} d_i^k \log\left[D\left(E(x_k)\right)\right]\right)\right) \quad (2)$$

In eq. (2), d_i^k is the true label of the current image and θ_S indicates the variable of the shared encoder. When guaranteeing that the global features of an image include some local features of the image as probable, it is also essential to guarantee that the local features of the image do not include those global features as much as promising. From this, the adversarial MTL model adopts orthogonal restrains to penalize redundant features and directs the encoder to capture features in multiple scales. Likewise, the loss function comprises the orthogonal restrain loss term l_O, as defined in Eq. (3).

$$l_O = \sum_{k=1}^{K} \|S_k P_k\|_F^2 \quad (3)$$

The major aim of the MTL is to differentiate the AA conditions of the multiple individuals under the different types of hair losses. The global encoder is applied to learn the common features (global features) between images from various classes. The merit of using the global encoder is that because each image traverse through the global encoder, the global encoder learns enriched semantic features. The discriminator assigned by the adversarial MTL model guarantees that the training sample of the global encoder is as independent as promising from the image source. But, a local encoder is assigned for all classes of AA images to learn the semantic features associated with the local feature. The presence of orthogonal restrains creates the training sample of the local encoder as relevant to the classification as probable. At last, the classifier is employed for AA identification. The input of the classifier is a feature representation obtained by the global feature and the local features of the image. Also, the outcome is the classification result.

3.2.2 Image Encoder

The underlying adversarial MTL model utilizes an LSTM encoder to encode images. It is assumed that it only takes the global features of the image and neglects the local features of the image to some extent. So, an Atrous convolution merged with LSTM is used to encode images, utilizing not only the global features of the image for classification but also the local features of multiple scales of the image. The architecture of this encoder is illustrated in Figure 4, which capotes local image features of multiple scales from the FRCNN encoder and concurrently captures global features of the image from an LSTM encoder and merges these 2 features to produce an entirely local or global feature representation.

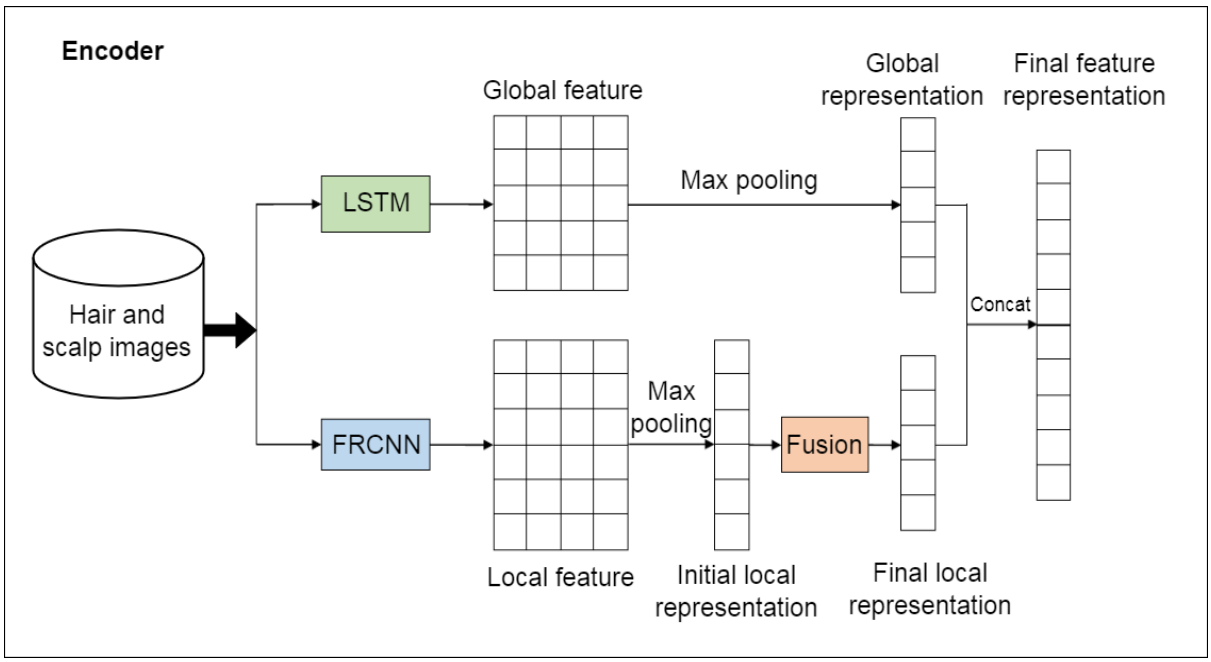

Figure 4. Architecture of the FRCNN-LSTM Encoder

A. Global Feature Extraction using LSTM

This encoder utilizes LSTM to capture the global features of an image and obtain the global representation of the image

features. The LSTM includes 3 gate control strategies such as forget gate, input gate and output gate. Meanwhile, it adopts the choice of dependent data on cell state control, which efficiently prevents the issue of gradient explosion and gradient disappearance. Its architecture is depicted in Figure 5.

The presence of the forget gate is to compute the degree of forgetting of the data flow before the ongoing cell. The determination is defined in Eq. (4):

$$f_t = \sigma\left(W_f \cdot [h_{t-1}, x_t] + b_f\right) \quad (4)$$

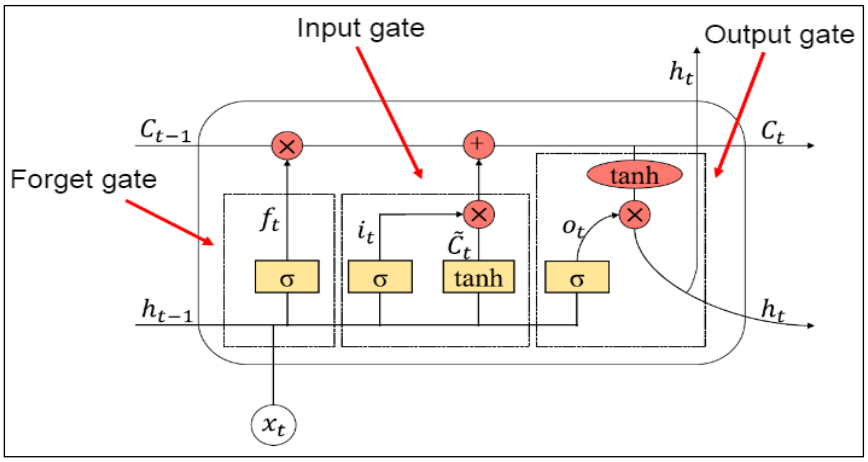

Figure 5. Architecture of LSTM Cell

The role of the input gate is to estimate how much present data is included in the data flow. The determination is defined in Eqns. (5) and (6):

$$i_t = \sigma(W_i \cdot [h_{t-1}, x_t] + b_i) \quad (5)$$

$$\tilde{C}_t = tanh(W_C \cdot [h_{t-1}, x_t] + b_C) \quad (6)$$

After the data traverse through the input gate and the forget gate, the LSTM fine-tunes the cell state to determine the outcome of the ongoing LSTM cell and pass it to the consecutive LSTM cell. The determination is defined in Eq. (7):

$$C_t = f_t * C_{t-1} + i_t * \tilde{C}_t \quad (7)$$

The output gate merges the present input and cell state to compute the result of the present LSTM cell. The computation is defined in Eqns. (8) and (9):

$$o_t = \sigma(W_o \cdot [h_{t-1}, x_t] + b_o) \quad (8)$$

$$h_t = o_t * tanh(C_t) \quad (9)$$

The function of this encoder to capture the global features of the image and create the global feature representation is illustrated in Figure 6(a). The initial image is input to the initial LSTM cell and the result gets the image feature of the present period and is sent to the consecutive LSTM cell. This process is repeated for all subsequent images until all features traverse through the LSTM cell and obtain their related present image features.

Because the input of the present period of the LSTM contains the result of the past period, the result of the final period is utilized as the global representation of the feature, as portrayed in Figure 6(b).

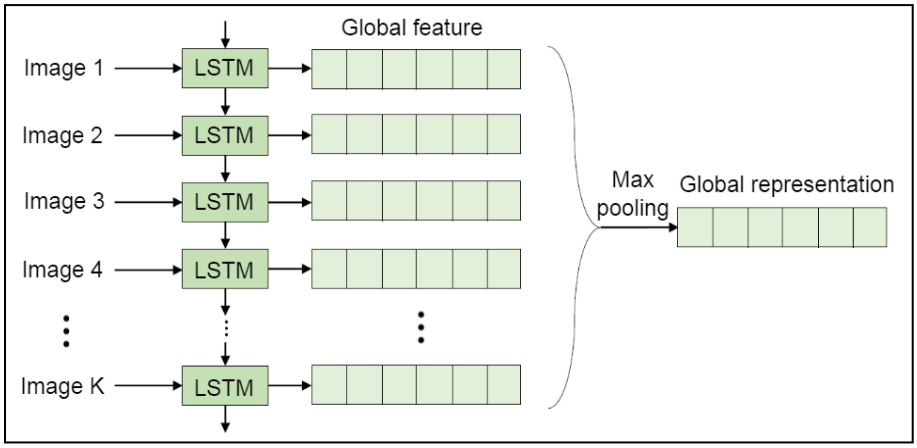

(a)

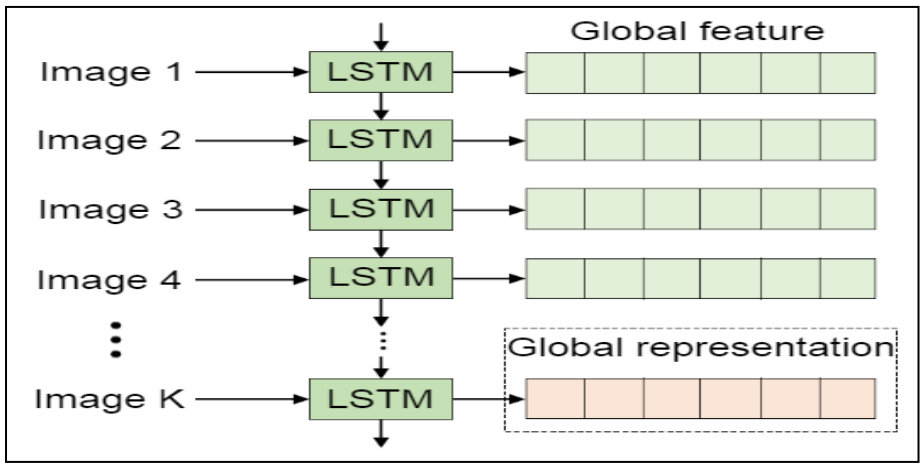

(b)

Figure 6. Global Feature Extraction and Representation using LSTM

B. Multi-dimensional Local Feature Extraction using FRCNN

FRCNN extracts local features of images by analyzing the pixels of the image via a convolution kernel. By considering color, texture and shape characteristics in the image, 3, 4 and 5 dimensions of convolution kernels are decided to capture the local features of the image on multiple scales. The determination is defined in Eq. (10):

$$c_i^r = f\left(F \cdot V\left(w(i{:}\, i+r-1)\right) + b\right) \quad (10)$$

In Eq. (10), F is the convolution kernel of $r * k$ dimension. In this study, the dimension of r is assigned to 3, 4, 5 and k refers to the size of the feature vector, f is the ReLU activation factor, $V\left(w(i{:}\, i+r-1)\right)$ defines that there are r feature vectors from i^{th} image to the $(i+r-1)^{th}$ image in the database and c_i^r is the i^{th} local feature of the image obtained by the convolution kernel with width r. The operation of this encoder to obtain the local features of the image and provide the local representations of the image is portrayed in Figure 7.

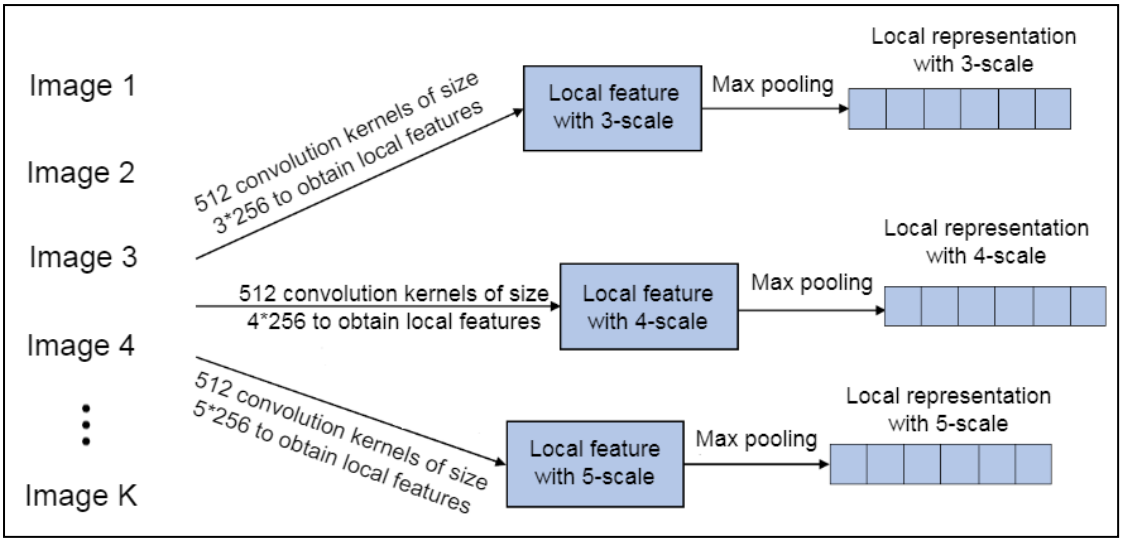

Figure 7. Multi-dimensional Local Feature Extraction and Representation using FRCNN

C. Concatenation of Local and Global Representations of Images

In the process explained above, the images have been provided to the LSTM and multi-scale FRCNN encoder to get the global and local representations of the image features. After that, such two outcomes are fused to create the entire local or global feature representation. In contrast, such 2 feature representations are not equal dimensions. So, the result of the LSTM network is given to the $tanh$ activation function and the feature dimensions of all scales are limited in the range $(-1,1)$, whereas the activation function utilized in the FRCNN is the ReLU. For the classification of AA conditions, the classifier can simultaneously learn the feature representations acquired by the 2 encoders.

To guarantee that the local and global data contained in the feature representations are in an identical state, concatenation is performed after the feature representations acquired by FRCNNs at 3 distinct scales. Further, the concatenated local representation is fused with the global representation to get the absolute result of the image encoder. At last, the resultant feature representation acquired from the result of the global encoder and the result of the local encoder is fed to the softmax classifier after the number of fully connected layers for minimizing the dimensionality. Also, this model is trained based on the Stochastic Gradient Descent (SGD) and the classifier loss is described as Eq. (12).

$$l(\hat{y}, y) = -\sum_{i=1}^{N}\sum_{j=1}^{C} y_i^j \log\left(\hat{y}_i^j\right) \quad (11)$$

$$l_C = \sum_{k=1}^{K} \alpha_k l\left(\hat{y}^{(k)}, y^{(k)}\right) \quad (12)$$

Thus, this MT-FRCNN-LSTM model can improve the accuracy of identifying and classifying the three different classes of AA: mild, moderate and severe with the help of both hair and scalp images.

4. EXPERIMENTAL RESULTS

This section investigates the effectiveness of the MT-FRCNN-LSTM model by executing it in MATLAB 2017b using figaro1k and dermnet databases (discussed in Section 3.1). In this experiment, 70% of images are taken for training and the remaining 30% of images are taken for testing. Additionally, a comparative analysis is presented to demonstrate its effectiveness compared with the classical models based on the different evaluation metrics. The considered classical models are FRCNN [8], ImageNet-VGG-f [18], SVM [22], HDM-Net-SVM [23], EfficientDet [25], YOLOv4 [25] and DetectoRS [25].

4.2 Accuracy

It is the proportion of exact categorization over the total images analyzed.

$$Accuracy = \frac{True\ Positive\ (TP) + True\ Negative\ (TN)}{TP + TN + False\ Positive\ (FP) + False\ Negative\ (FN)} \quad (13)$$

In Eq. (13), the number of healthy images correctly classified as positive (healthy) is TP, while the number of AA images correctly classified as negative (AA) is TN. In addition, FP denotes the number of AA images classified as healthy, whereas FN denotes the number of healthy images classified as AA.

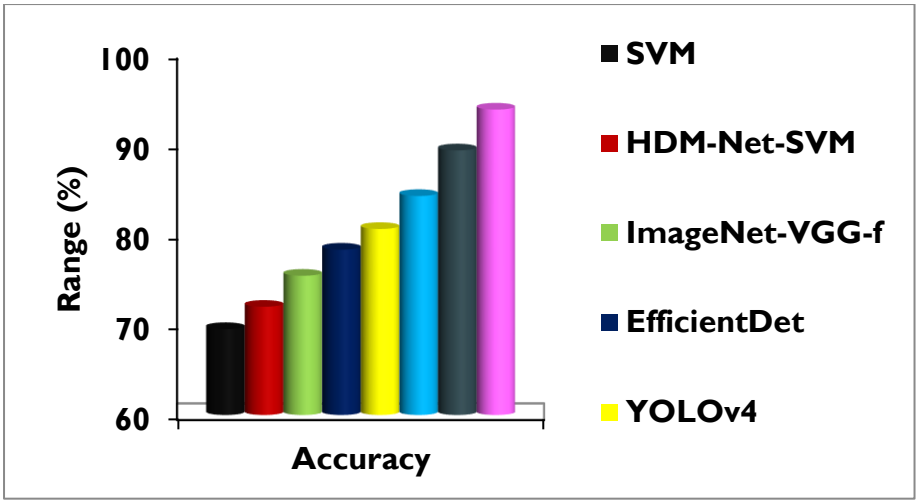

Figure 8. Comparison of Accuracy

Figure 8 displays the accuracy (in %) realized by the different AA identification models. It addresses that the accuracy of the MT-FRCNN-LSTM is 34.84% greater than the SVM, 30.2% greater than the HDM-Net-SVM, 24.28% greater than the ImageNet-VGG-f, 19.71% greater than the EfficientDet, 16.33% greater than the YOLOv4, 11.31% greater than the DetectoRS and 5.04% greater than the FRCNN models. This is because of handling both local and global features from the hair and scalp images at multiple scales.

4.3 Precision

It is determined as:

$$Precision = \frac{TP}{TP+FP} \quad (14)$$

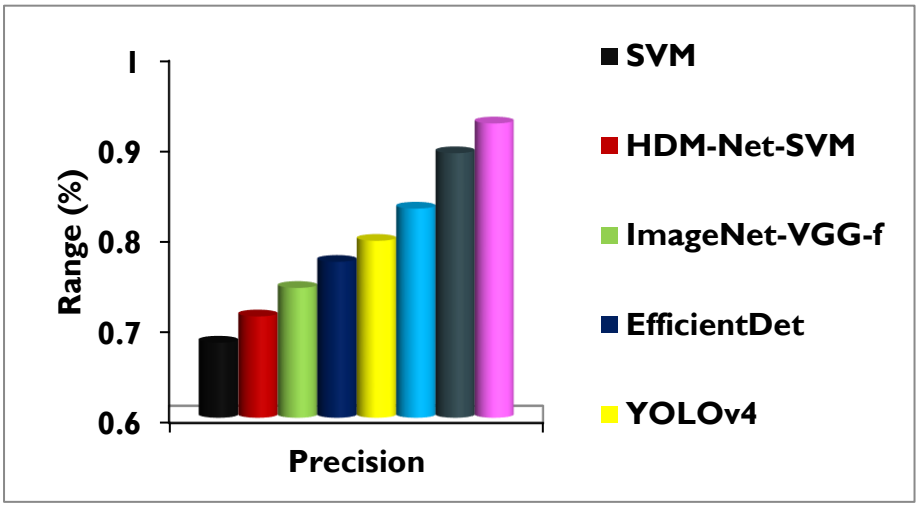

Figure 9. Comparison of Precision

Figure 9 shows the precision achieved by the different AA identification models using hair and scalp images. It notices that the precision of the MT-FRCNN-LSTM model is 35.54% higher than the SVM, 30.05% higher than the HDM-Net-SVM, 24.55% higher than the ImageNet-VGG-f, 19.88% higher than the EfficientDet, 16.37% higher than the YOLOv4, 11.37% higher than the DetectoRS and 3.7% higher than the FRCNN models because of capturing both local and global features from the hair and scalp images at different scales.

4.4 Recall

It is determined as:

$$Recall = \frac{TP}{TP+FN} \quad (15)$$

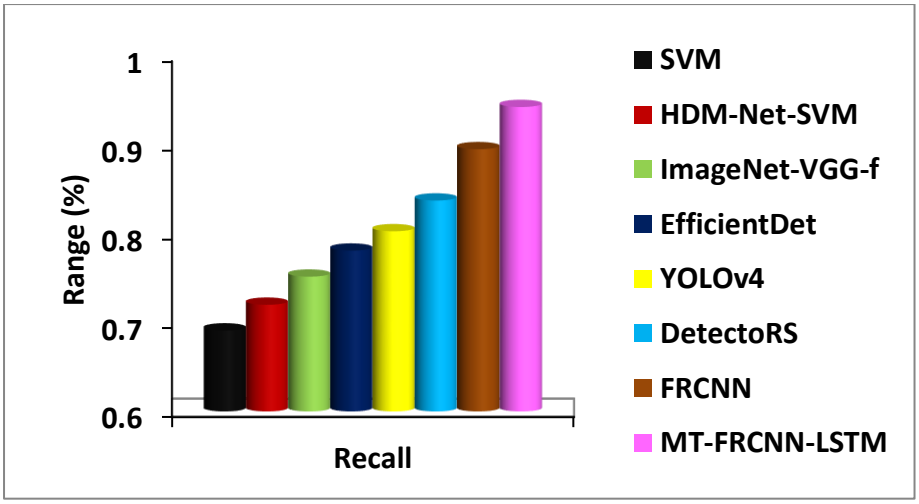

Figure 10. Comparison of Recall

Figure 10 portrays the recall for various AA identification models. It observes that the recall of the MT-FRCNN-LSTM model is 36.4% larger than the SVM, 30.94% larger than the HDM-Net-SVM, 25.43% larger than the ImageNet-VGG-f, 20.72% larger than the EfficientDet, 17.44% larger than the YOLOv4, 12.58% larger than the DetectoRS and 5.31% larger than the FRCNN models owing to the learning both local and global features from the hair and scalp images of various AA levels at different scales.

4.5 F-measure

It is calculated by

$$F - measure = \frac{2 \times Precision \times Recall}{Precision + Recall} \quad (16)$$

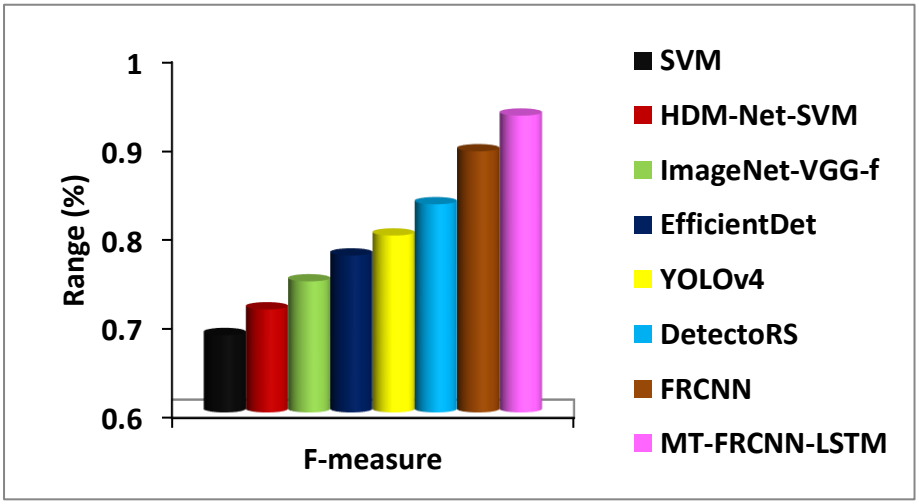

Figure 11. Comparison of F-measure

Figure 11 depicts the f-measure values for various models applied to identify and diagnose AA conditions. It indicates that the f-measure of the MT-FRCNN-LSTM model is 35.96% superior to the SVM, 30.49% superior to the HDM-Net-SVM, 24.98% superior to the ImageNet-VGG-f, 20.3% superior to the EfficientDet, 16.91% superior to the YOLOv4, 11.97% superior to the DetectoRS and 4.5% superior to the FRCNN models due to the extraction of both local and global features from the hair and scalp images at different scales.

5. CONCLUSION

In this study, the MT-FRCNN-LSTM model was presented for identifying and diagnosing various levels of AA by learning both hair and scalp images together. Primarily, the hair and scalp image databases were acquired from the openly available sources. Then, such images were passed to the LSTM encoder and the FRCNN encoder to concurrently obtain the global

and local feature representations from the images at different scales. Once both feature representations were obtained, concatenation was performed to fuse such features and get the absolute feature representation. Further, the absolute feature representation was passed to the softmax classifier after the fully connected layer to identify and classify the different levels of AA efficiently. At last, the experimental outcomes proved that the MT-FRCNN-LSTM model on hair and scalp image databases has a 93.82% accuracy compared to the other models for AA identification and diagnosis. As a result, it supports physicians to diagnose patients who suffer from AA earlier.

REFERENCES

[1] Trüeb, R. M., & Dias, M. F. R. G. (2018). Alopecia areata: a comprehensive review of pathogenesis and management. *Clinical Reviews in Allergy & Immunology*, *54*(1), 68-87.

[2] Lintzeri, D. A., Constantinou, A., Hillmann, K., Ghoreschi, K., Vogt, A., & Blume-Peytavi, U. (2022). Alopecia areata–Current understanding and management. *Journal der Deutschen Dermatologischen Gesellschaft*, *20*(1), 59-90.

[3] Rajput, R. (2015). Understanding hair loss due to air pollution and the approach to management. *Hair Ther Transplant*, *5*(133), 1-5.

[4] Su, J. P., Chen, L. B., Hsu, C. H., Wang, W. C., Kuo, C. C., Chang, W. J., ... & Lee, D. H. (2018). An intelligent scalp inspection and diagnosis system for caring hairy scalp health. In *IEEE 7th Global Conference on Consumer Electronics*, pp. 507-508.

[5] Gulati, R., Nijhawan, M., Agarwal, S., Gupta, I., Soni, S., Goyal, V., ... & Mathur, D. (2015). Prevalence of scalp disorders among outpatients attending dermatology department in a semi-urban setup: a cross sectional observational study. *Journal of Evolution of Medical and Dental Sciences*, *4*(38), 6620-6624.

[6] Harningtyas, C. D., Ervianti, E., Astari, L., Anggraeni, S., & Widia, Y. (2022). A case report of tinea capitis in children: utility of trichoscopy. *Berkala Ilmu Kesehatan Kulit dan Kelamin*, *34*(1), 66-72.

[7] Legiawati, L., Santoso, I. D., & Lubis, F. F. (2021). Comparison between clinical diagnosis with and without dermoscopy in the assessment of hair disorders. *Journal of Pakistan Association of Dermatologists*, *31*(2), 201-205.

[8] Chang, W. J., Chen, L. B., Chen, M. C., Chiu, Y. C., & Lin, J. Y. (2020). ScalpEye: A deep learning-based scalp hair inspection and diagnosis system for scalp health. IEEE Access, 8, 134826-134837.

[9] Alshahrani, A. A., Al-Tuwaijri, R., Abuoliat, Z. A., Alyabsi, M., AlJasser, M. I., & Alkhodair, R. (2020). Prevalence and clinical characteristics of alopecia areata at a tertiary care center in Saudi Arabia. *Dermatology Research and Practice*, *2020*, 1-4.

[10] Fricke, A. C. V., & Miteva, M. (2015). Epidemiology and burden of alopecia areata: a systematic review. *Clinical, cosmetic and investigational dermatology*, *8*, 397-403.

[11] Pratt, C. H., King, L. E., Messenger, A. G., Christiano, A. M., & Sundberg, J. P. (2017). Alopecia areata. *Nature reviews Disease primers*, *3*(1), 1-17.

[12] Ocampo-Garza, J., & Tosti, A. (2019). Trichoscopy of dark scalp. *Skin appendage disorders*, *5*(1), 1-8.

[13] Gupta, A. K., Ivanova, I. A., & Renaud, H. J. (2021). How good is artificial intelligence (AI) at solving hairy problems? A review of AI applications in hair restoration and hair disorders. *Dermatologic Therapy*, *34*(2), 1-9.

[14] Daniels, G., Tamburic, S., Benini, S., Randall, J., Sanderson, T., & Savardi, M. (2021). Artificial Intelligence in hair research: a proof-of-concept study on evaluating hair assembly features. *International Journal of Cosmetic Science*, *43*(4), 405-418.

[15] Jhong, S. Y., Yang, P. Y., & Hsia, C. H. (2022). An Expert Smart Scalp Inspection System Using Deep Learning. *Sensors and Materials*, *34*(4), 1265-1274.

[16] Alarcón-Soldevilla, F., Hernández-Gómez, F. J., García-Carmona, J. A., Carreño, C. C., Grimalt, R., Vañó-Galvan, S., ... & Arcas-Tunez, F. (2021). Use of artificial intelligence as a predictor of the response to treatment in alopecia areata. *Iproceedings*, 7(1), 1-2.

[17] Nabahhin, A., Aloun, A. A., & Almurshidi, S. H. (2017). Hair loss diagnosis and treatment expert system. *International Journal of Engineering and Information Systems*, *1*(4), 160-169.

[18] Wang, W. C., Chen, L. B., & Chang, W. J. (2018). Development and experimental evaluation of machine-learning techniques for an intelligent hairy scalp detection system. *Applied Sciences*, *8*(6), 1-28.

[19] Lee, S., Kim, B. J., Lee, C. H., & Lee, W. S. (2019). Topographic phenotypes of alopecia areata and development of a prognostic prediction model and grading system: a cluster analysis. *JAMA*

dermatology, *155*(5), 564-571.

[20] Seo, S., & Park, J. (2020). Trichoscopy of alopecia areata: hair loss feature extraction and computation using grid line selection and eigenvalue. *Computational and Mathematical Methods in Medicine*, *2020*, 1-9.

[21] Fatima, R., Arif, T., & Shivakumar, V. (2020). Clinical, dermoscopic and histopathological assessment in patients of alopecia areata: a hospital based cross-sectional study. *Journal of Pakistan Association of Dermatologists*, *30*(2), 256-260.

[22] Ibrahim, S., Noor Azmy, Z. A., Abu Mangshor, N. N., Sabri, N., Ahmad Fadzil, A. F., & Ahmad, Z. (2020). Pre-trained classification of scalp conditions using image processing. *Indonesian Journal of Electrical Engineering and Computer Science*, *20*(1), 138-144.

[23] Zhang, L., Man, Q., & Cho, Y. I. (2021). Deep-learning-based hair damage diagnosis method applying scanning electron microscopy images. *Diagnostics*, *11*(10), 1-12.

[24] Shakeel, C. S., Khan, S. J., Chaudhry, B., Aijaz, S. F., & Hassan, U. (2021). Classification framework for healthy hairs and alopecia areata: a machine learning (ml) approach. *Computational and Mathematical Methods in Medicine*, *2021*, 1-10.

[25] Kim, M., Kang, S., & Lee, B. D. (2022). Evaluation of automated measurement of hair density using deep neural networks. *Sensors*, *22*(2), 1-10.

[26] http://projects.i-ctm.eu/it/progetto/figaro-1k

[27] http://www.dermnet.com/dermatology-pictures-skin-disease-pictures